

# ELASTIC AND ELASTIC-PLASTIC ANALYSIS OF AEROSOL CANS BASE UNDER INTERNAL PRESSURE

Ragba M. Abdussalam Abotwerat

University of Sebha Faculty of Engineering and Technology Brack Al-Sahti  
P.O Box 68

## المخلص

تم في هذا البحث دراسة السلوك المرن للندن لقاعدة علب بخاخ العرق عندما تتعرض لضغط داخلي في بعدين وثلاث أبعاد في حالتها سلوك المادة المرنة المرنة والمرن اللدن. يعتبر تحليل العناصر المحدودة أداة قوية لأجاد الإجهاد والانفعال المتوقع و سلوك الإزاحة للعناصر المكونة في التركيب. استخدمت طريقة تحليل العناصر المحدودة المرنة اللدن من أجل تطوير الفهم الشامل للطريقة في عملية الخضوع التي تحدث أثناء تركيب الأجزاء الميكانيكية للآلة "القبة المعكوسة" (ميزة السلامة الصلبة حيث تعاني القاعدة من الانبعاج اللدن المرنة عندما تتعرض لضغط اقل من ضغط الانفجار) وانهارها نتيجة لحمولة الضغط الداخلي وكيف يتأثر شكلها نتيجة لذلك. كما تم القيام بتجارب في الورشة لاستنتاج سلوك الانبعاج والانهيال وتبين وجود اتفاق معقول بين البيانات التجريبية والنتائج التي استنتجت من طريقة العناصر المحدودة. أجريت التحاليل في هذا البحث باستخدام برنامج العناصر المحدودة لشركة ميكروسوفت وندز (Microsoft Windows NT) (ELFEN VERSION 3.0.4) أتاح البرنامج المعالجة المسبقة والتحليل ومراحل المعالجة اللاحقة ضمن عملية تطبيق واحدة. يمكن أن يستعمل البرنامج لتشكيل عدد كبير من الحالات شاملا الانبعاج والتشوه اللدن والتشكيل وتحليل الإجهاد وغيرها.

## ABSTRACT

This paper describes the results of a study of elastic and elastic-plastic behavior of the aerosol can base subjected to internal pressure in 2-D and 3-D. Elastic-perfectly-plastic and work hardening material model is assumed.

Finite element analysis (FEA) is a powerful tool for predicting stress, strain and displacement behavior of components and structures. Elastic and elastic-plastic (FEA) has been used in this study to develop a thorough understanding of the mechanisms of yielding, 'dome reversal' (an inherent safety feature, where the base suffers elastic-plastic buckling at a pressure below the burst pressure) and collapse due to internal pressure loading and how these are affected by geometry. Experimental verification of the buckling and collapse behaviors has also been carried out in this study and there is reasonable agreement between the experimental data and the numerical predictions.

The analysis was completed using ELFEN Version 3.0.4 [1], finite element program for Microsoft Windows NT. The program allows pre-processing, analysis and post-processing stages to be completed within a single application. The program can be used to model a large number of situations including buckling, plastic deformation, forming and stress analysis problems, etc.

**KEYWORDS:** Finite element analysis; Elastic-plastic behavior; Can base.

## INTRODUCTION

An aerosol can is a thin-walled cylinder with a complex shape which limits the amount of 'design' that can be undertaken using simple thin cylinder equations to

estimating the burst pressure of the can. Aluminum aerosol cans are a particular form of thin-walled cylinder with a complex shape consisting of truncated cone top, parallel cylindrical section and inverted dome base. They are manufactured in one piece by a reverse-extrusion process, which produces a vessel with a variable thickness from 0.31 mm in the cylinder up to 1.31 mm in the base for a 53 mm diameter can. Very little research has been conducted into the design of these more complex shapes. Patten [2] developed a program to predict the height and thickness variation in the first stage of the back-extrusion process for aluminum aerosol cans. In 1999, Benjamin [3] studied the computational strategies for the design and optimization of three-piece steel food cans. In reality, an aerosol can is subjected to a number of loading patterns including internal pressure, axial and radial loading and although the behavior of a plain cylinder with constant wall thickness is well understood, what is required is an analysis method that can be used to accurately predict the elastic and elastic-plastic stresses and deformation of these cylinders due to internal pressure, axial and radial loading, as well as providing details of the modes and behavior during failure, including buckling. Finite element analysis (FEA) is such a powerful and comprehensive analysis method and has been used comprehensively in this paper, supported by experimental validation.

The thickness profile of an aerosol can is such that a number of design requirements have to be met:

Cylinder	Must be thick enough to withstand bursting due to overpressure Must be thick enough to withstand radial buckling during bundling/packaging Must be thick enough to avoid axial buckling/collapse under compressive axial load during manufacture and charging
Base	Must be thick enough to withstand bursting due to overpressure Must be thin enough to facilitate 'dome reversal' at a specified pressure below the burst pressure
Top	Must be thick enough to withstand bursting due to overpressure Must be thick enough to avoid collapse under compressive axial load during manufacture and charging

The results presented here are part of an analytical study of the can base subjected to internal pressure load in the elastic analysis and in elastic-plastic analysis. Also the elastic-plastic analysis of different loading conditions was described. The 3-D model of the can base was produced to product the deformation pressure.

## GEOMETRIES

A typical geometry is shown in Figure (1). The basic shape of the component is a two-dimensional can base having uniform thickness. Six geometries (G1 to G6) have been considered in this analysis and the relevant geometry parameters are listed in Table (1). A detailed investigation of G4 is described. A summary of the results is given for the other geometries, using elastic –perfectly –plastic and actual aluminum material data models.

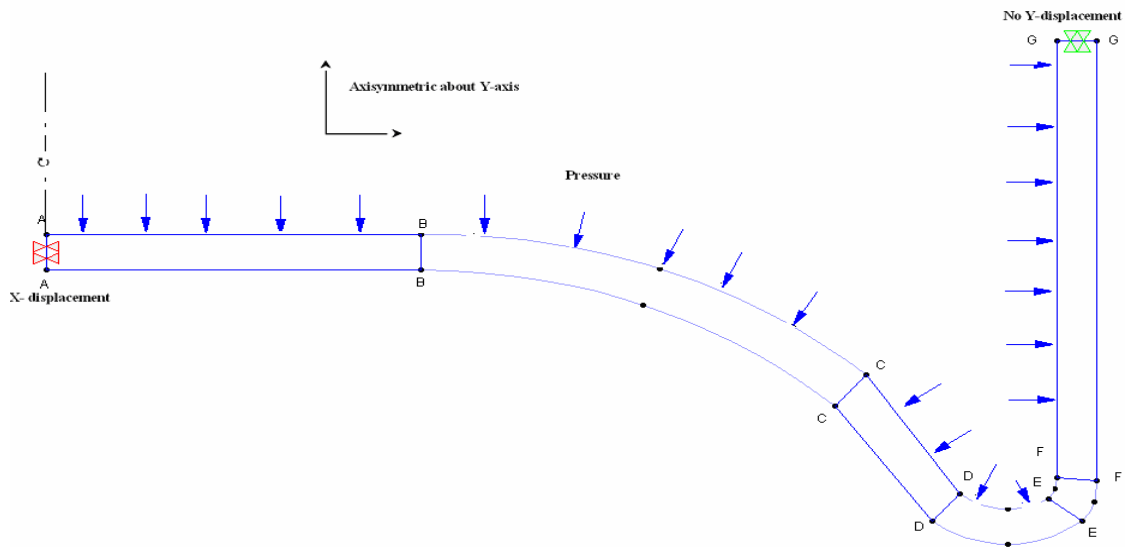


**Figure 1: Finite element model**

**Table 1: Geometry parameters**

Geometries	H (mm)	t (mm)	L (mm)	R(mm)	r (mm)	$\theta$ (degree)
G1	8.5	0.4	8.924	13.75	1.50	87.8°
G2	8.5	0.6	8.924	13.75	1.62	86.7°
G3	8.5	0.8	8.924	13.75	1.93	67.3°
G4	8.5	1.0	8.924	13.75	2.74	50.5°
G5	8.5	1.2	8.924	13.75	3.20	30.4°
G6	8.5	1.4	8.924	13.75	3.20	25.2°
G7	8.5	vary	8.924	14.13	3.23	64.2°

## LOADING AND BOUNDARY CONDITIONS

Elastic finite element calculation has been performed for pressure loads applied uniformly on the inner surface of the base. For the elastic-plastic analysis the loading was applied incrementally. The model is constrained in the X direction along the plane  $X = 0$  and constrained in Y direction along the plane  $Y = 0$ .

## MATERIALS MODELS

The material assumed for the elastic analysis is aluminum 1050 the mechanical properties are given in Table (2). For the elastic-plastic analysis an elastic-perfectly – plastic and actual aluminium material models was assumed. The von Mises effective stress criterion and Newton-Raphson iteration method was used [4].

**Table 2: Mechanical properties of 1050 Aluminium**

Mechanical material properties	Value
Density, $\rho$ (kg/m <sup>3</sup> )	2700
Young's modulus, E (GPa)	68.3
Poisson's ratio, $\nu$	0.33

## FINITE ELEMENT ANALYSIS

In both cases elastic and elastic-plastic maximum equivalent stress have been obtained. A typical mesh, using rectangular 8 noded axisymmetric isoparametric elements, is shown in Figure (2).

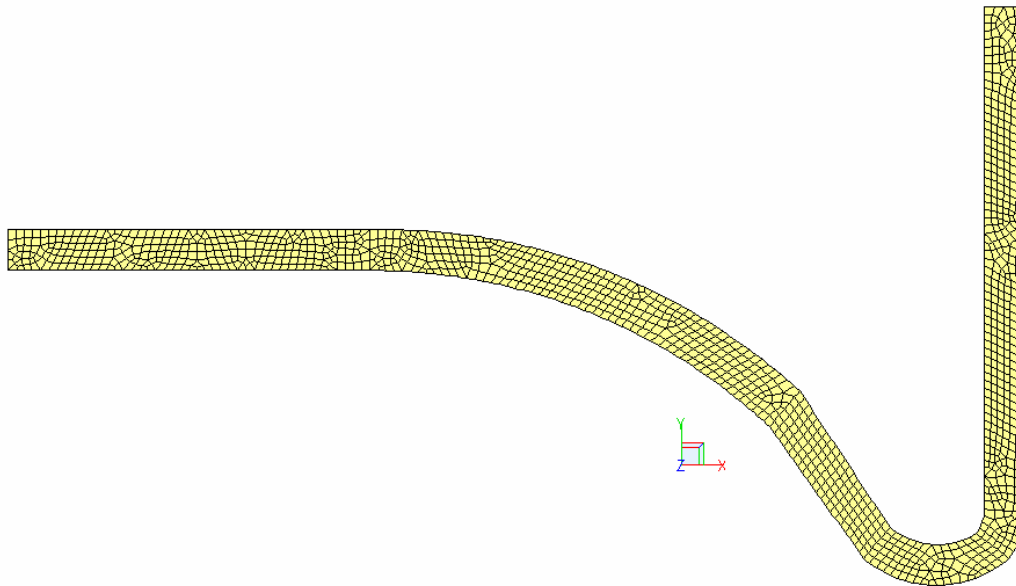


Figure 2: Finite element mesh for geometry G4

## RESULTS OF ELASTIC ANALYSIS

The contours of maximum principal stresses for geometry G4 under an internal pressure of 1 bar are presented. Elastic principal stress contour plots ( $\sigma_1$ ) for geometry G4 for an internal pressure of 0.1 MPa are presented in Figure (3)..

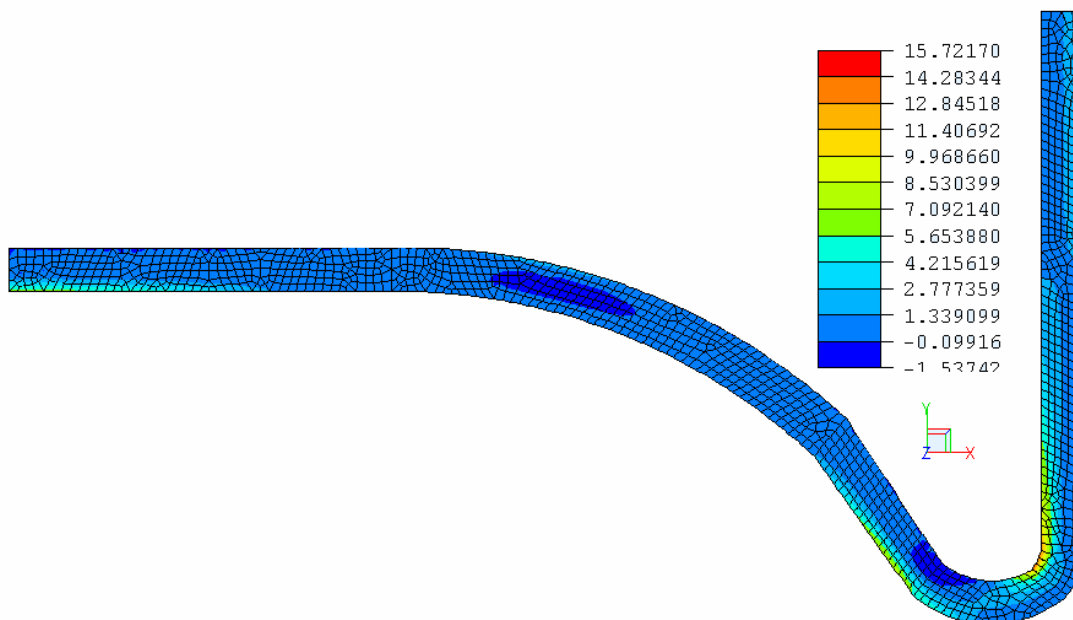
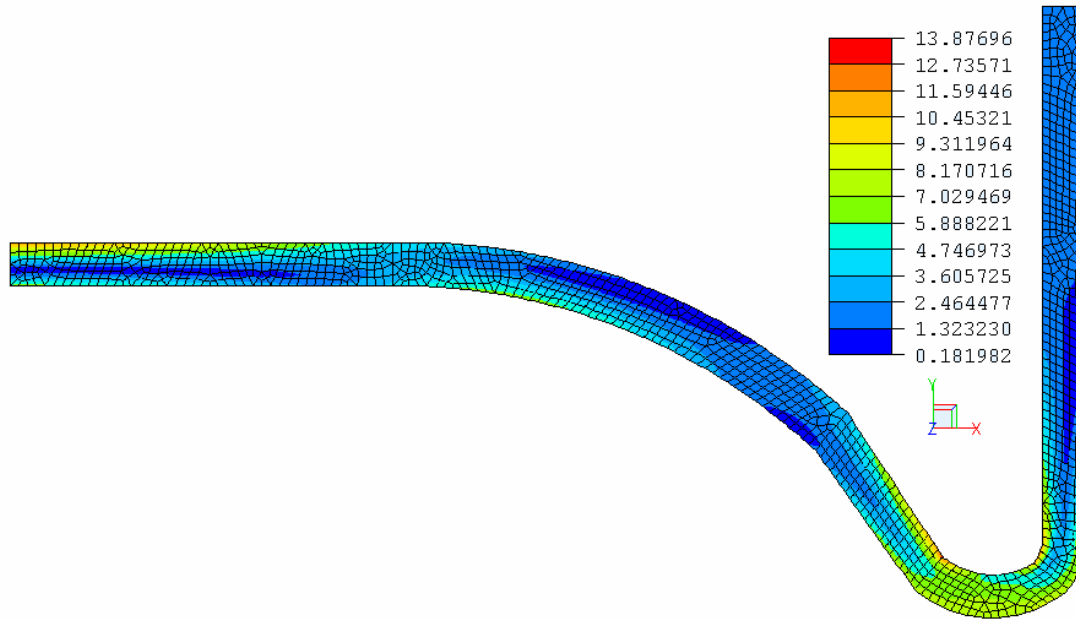


Figure 3: Stress contour plot for principal stresses ( $\sigma_1$ ) at internal pressure of 1 bar

It can be seen that  $\sigma_1$  has a maximum localized value of +15.72 MPa on the inside surface close to the intersection between the base and vertical sides (section EE in

Figure (1). Elsewhere,  $\sigma_1$  is reasonably uniform and of low value.  $\sigma_2$  Varies between +2.02 and -14.46 MPa with the maximum compressive value on the inside surface between sections CC and DD in Figure (1).  $\sigma_3$  varies between +9.26 and -11.43 MPa with a maximum tensile value close to section DD in Figure (1) and generally compressive stresses in the uniform base region,  $\sigma_1$  is the hoop stress,  $\sigma_2$  is the longitudinal stress and  $\sigma_3$  is the radial stress approximately

The von Mises equivalent stress contour plot, for  $p = 0.1$  MPa, is shown in Figure (4). The maximum equivalent stress is 13.88 MPa and it occurs on the inner surface close to point E in Figure (1).



**Figure 4: Stress contour plot for G4, at internal pressure of 1 bar**

The maximum elastic equivalent stress index,  $\hat{I}_{eq}$ , is obtained by dividing the maximum equivalent stress by the nominal stress:

$$\hat{I}_{eq} = \frac{(\sigma_{max})_{eq}}{(\sigma_{eq})_{nom}} \quad (1)$$

Where the nominal stress is found from:

$$(\sigma_{eq})_{nom} = \frac{1}{\sqrt{2}} \sqrt{[(\sigma_1 - \sigma_2)^2 + (\sigma_2 - \sigma_3)^2 + (\sigma_3 - \sigma_1)^2]} \quad (2)$$

and  $\sigma_1 = \frac{PD}{2t}$ ,  $\sigma_2 = \frac{PD}{4t}$ ,  $\sigma_3 = -\frac{P}{2}$ , D is the inside diameter.

Using  $p = 0.1$  MPa,  $D = 53$  mm and  $t = 1$  mm:

$\sigma_1 = 2.65$  MPa,  $\sigma_2 = 1.325$  MPa,  $\sigma_3 = -0.05$  MPa,  $(\sigma_{eq})_{nom} = 2.34$  MPa and hence  $\hat{I}_{eq} = 5.93$  MPa.

It is clear that yielding will occur here first at a pressure which is well below the yield pressure for the plain tube region of the can with 1 mm wall thickness, which is when  $(\sigma_{eq})_{nom} = 100$  MPa. Hence, scaling up these elastic results, first yield occurs when:

$$p_y = \frac{100}{13.88} \cdot 0.1 = 0.720 \text{ MPa} \quad \text{- for the base}$$

Compared with:

$$p_y = \frac{100}{2.34} \cdot 0.1 = 4.27 \text{ MPa} \quad \text{- for the plain tube}$$

The variation of  $\hat{I}_{eq}$  with wall thickness,  $t$ , is shown in Figure (5) it's clear from the chart that the maximum elastic equivalent stress index,  $\hat{I}_{eq}$  increased when the thickness decreased.

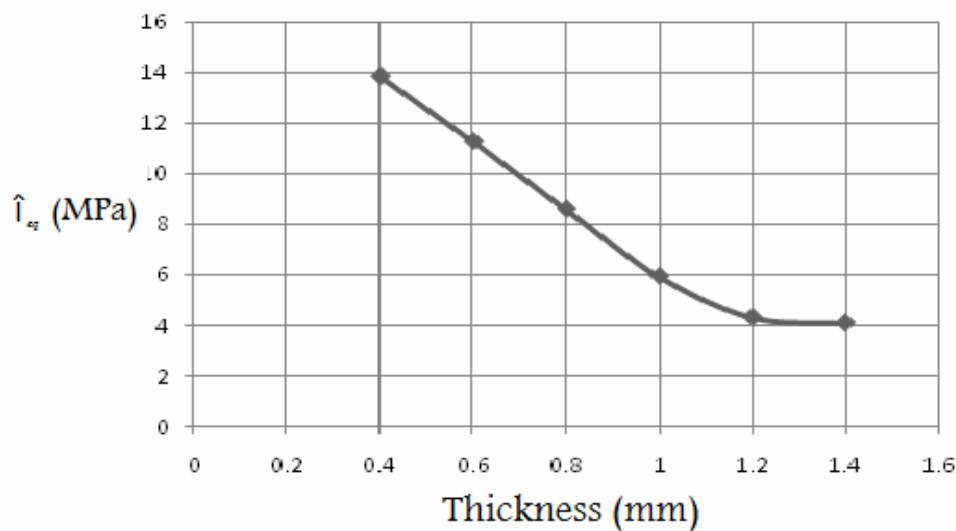


Figure 5: The relationship between elastic equivalent stress index and the wall thickness

## RESULTS OF ELASTIC-PLASTIC ANALYSIS

### Elastic-perfectly-plastic Model

The extent of the plastic zone for pressure load of 16 bar is shown in Figure (6). As a structure deforms a redistribution of stresses may take place Figures (7, 8) show the stress distribution of the can base around the inside and outside surface.

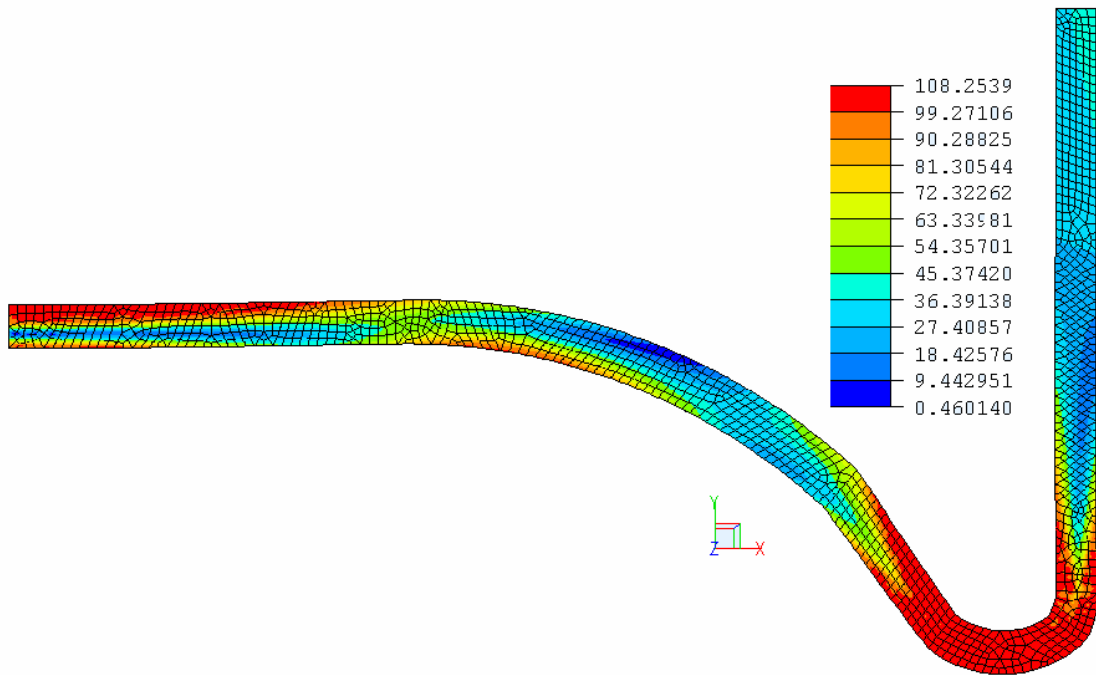


Figure 6: Von Mises stress contour plot at internal pressure of 16 bar

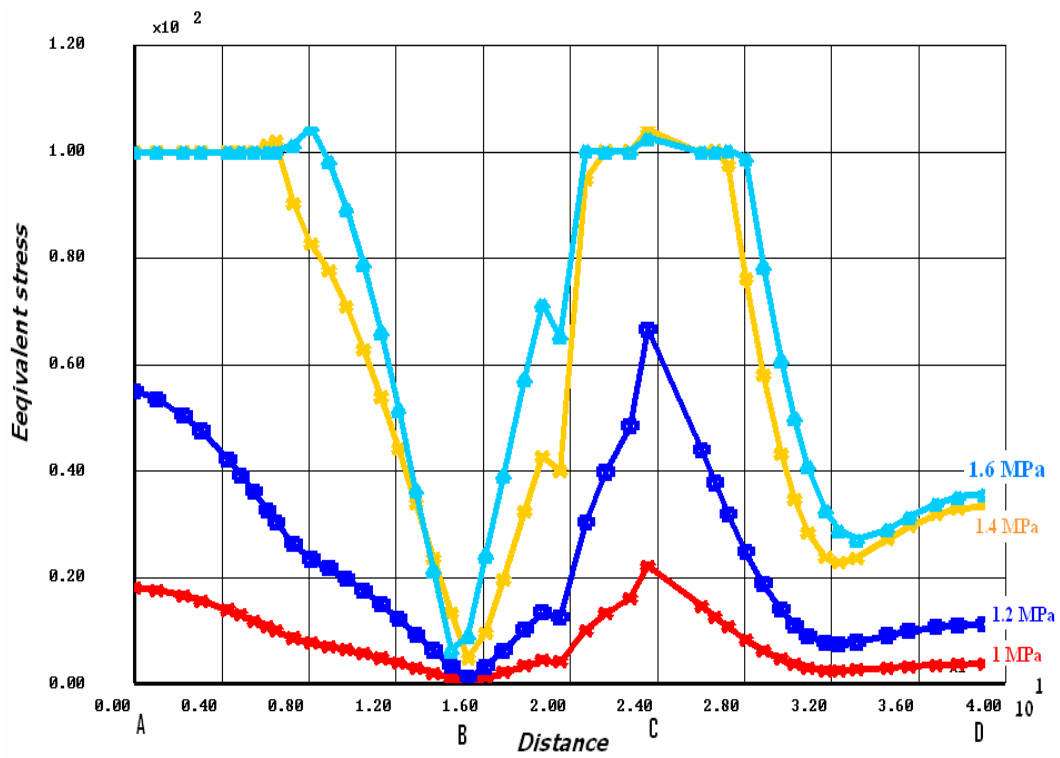


Figure 7: Stress distribution around inside surface

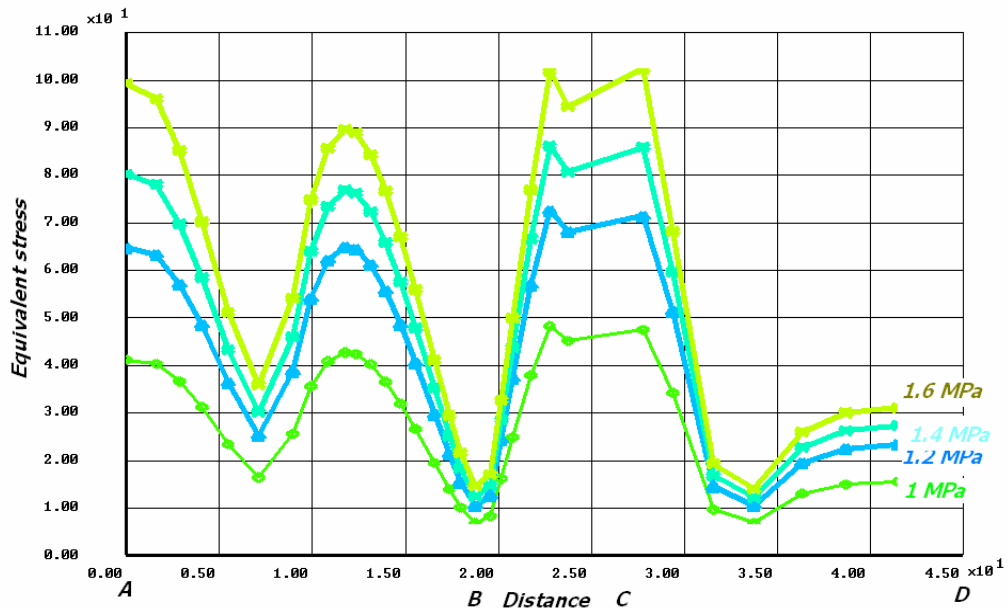


Figure 8: Stress distribution around outside surface

### Multi-linear Work-Hardening Model

The results of the analysis in work-hardening material are shown in Figure (10) to predict the stresses after collapse.

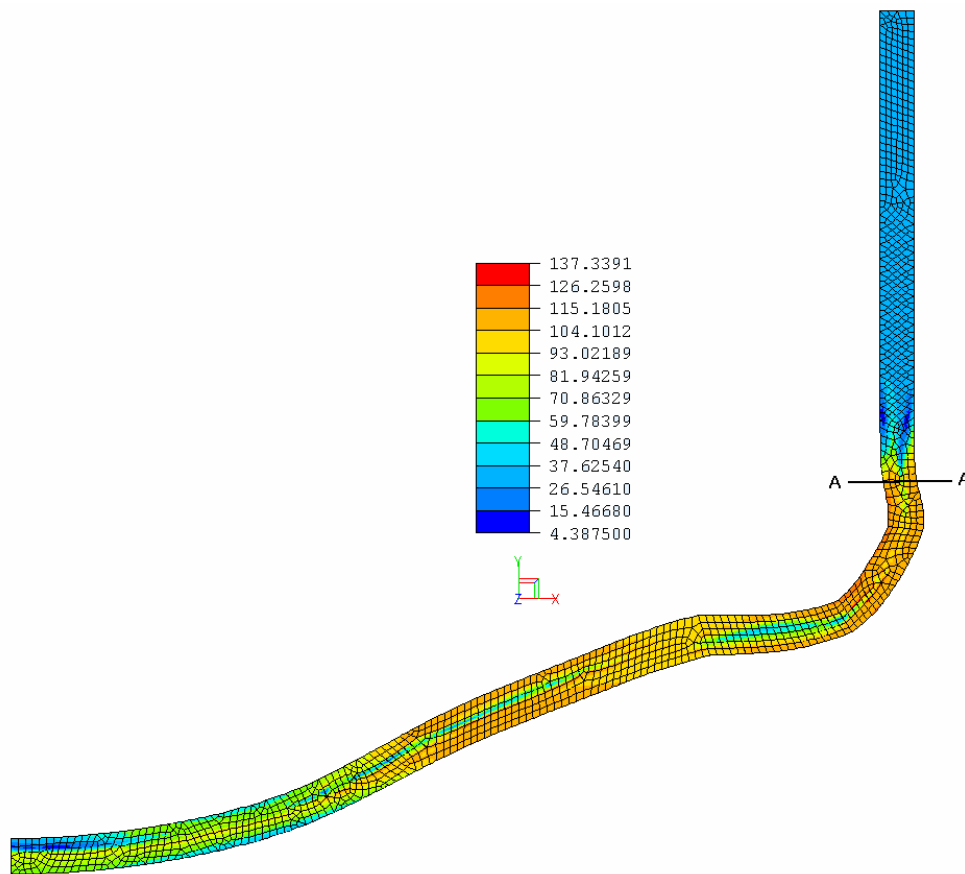


Figure 10: Von Mises stress contour (Post buckling, pressure 15.9 Bar)

### Effect of wall Thickness

The results of the analysis of different thickness (0.4, 0.6, 0.8, 1, 1.2 and 1.4 mm) are shown in Figure (11) below using the multi-linear hardening model. The EPP model was not considered because it is not realistic and was only included for  $t = 1$  mm for illustration. The variation in limiting pressure is reasonably linear the curve for collapse pressure shows a clear increase in slope with increasing thickness. This is important for material optimization.

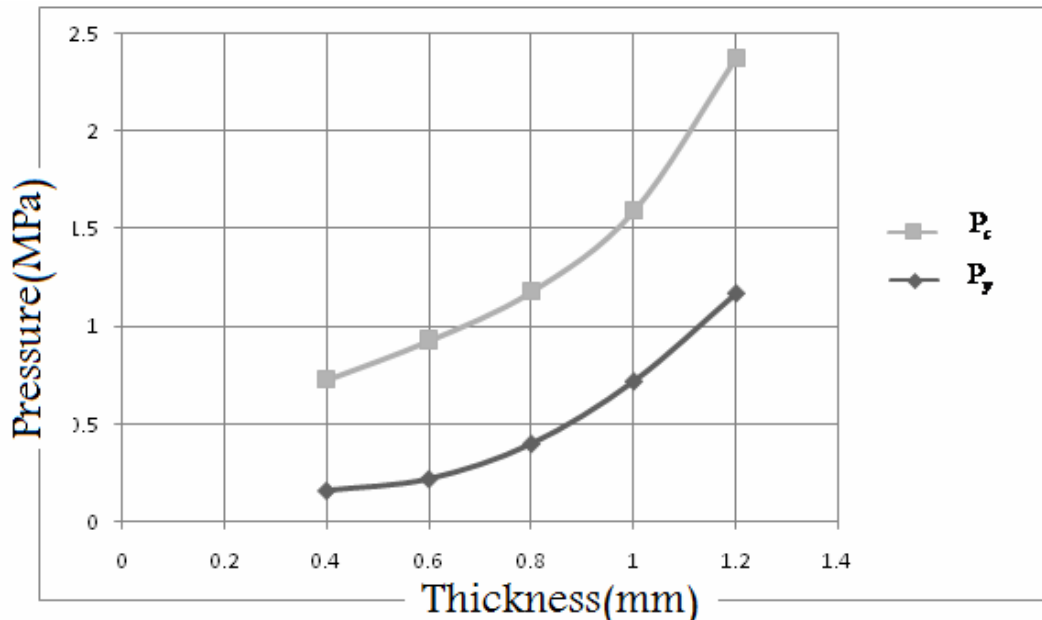


Figure 11: The relationship between thickness and collapse and first yield pressure

### Finite Element Result for Various Thicknesses

The finite element model for various thicknesses is shown in Figure (12). The results of the analysis in work-hardening material are shown as stress contours in Figure (13). The stresses predicted from the analysis are intended the region of high stress.

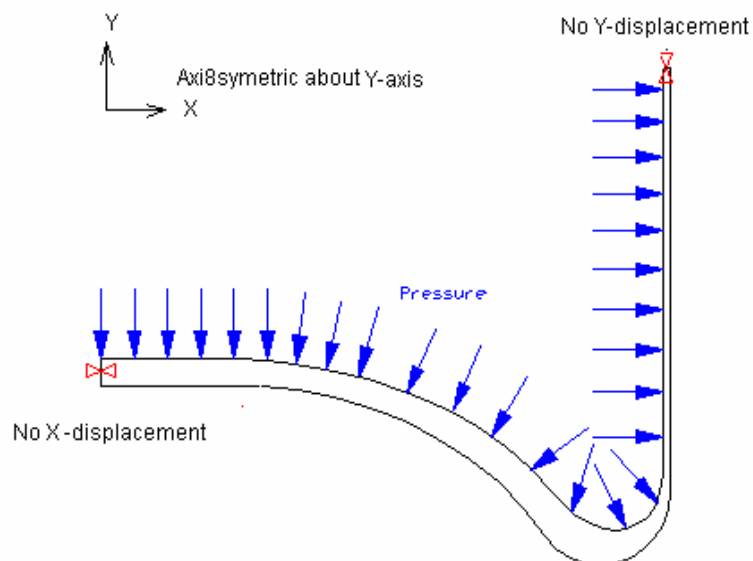
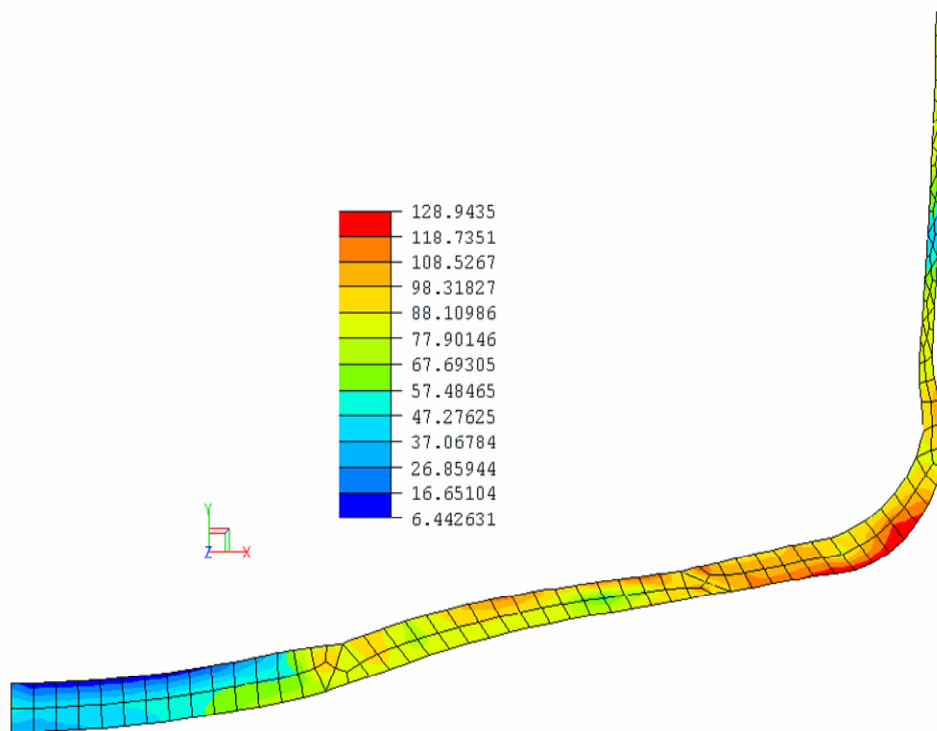


Figure 12: Finite element model



**Figure 13: Von Mises stress contour (Post buckling, pressure 15.3 Bar)**

### **THREE-DIMENSIONAL ANALYSIS OF PRESSURE LOADING**

This section describes all the parameters that must be taken into account in producing a finite element model to predict the actual failure and the limit load for the can base under internal pressure loading.

A three-dimensional finite element model was created. It was required to use a three-dimensional model because the lowest failure mode is seen experimentally to be unsymmetrical buckling of the can base. Additionally, due to the large deformations involved, it was required to use a geometrically non-linear analysis since the loading will change direction throughout the analysis [5]. This allows the pressure load to follow the deformation and remain normal to the applied surface as opposed to remaining in its initial direction. As with all non-linear finite element models, the loading must be incremented in small steps up to the required value and in this case an arc load function was used, this is because the load required to deform the base increases until the base begins to buckle, then decreases as the base deforms before increasing again when the base is fully deformed, until the can walls fail [6].

#### **Finite element model (pressure loading)**

A three-dimensional model was developed by rotating the model shown in Figure (12) through  $180^\circ$ , as shown in Figure (14) with FE Constraints to create a half model of the can. Only the lower section of the can was modeled since it was known from experimental evidence that unsymmetrical deformation would occur in this area. It was not possible to use an axisymmetric model due to this unsymmetrical buckling mode. The model was constrained along its line of symmetry in the X direction see Figure (14)

(plane ABCD). This does not allow X displacement of these elements, to model the can as symmetrical. The top section of the can was constrained in the Z direction (plane ADE) to simulate the gripping of the can in the pressure testing equipment. In reality the can is gripped at the shoulder during the pressure tests not in the midsection as in the model. Again, due to the large deformations, it was necessary to use a geometric non-linear analysis since the loading will change direction during the buckling process and the stiffness of the base changes significantly.

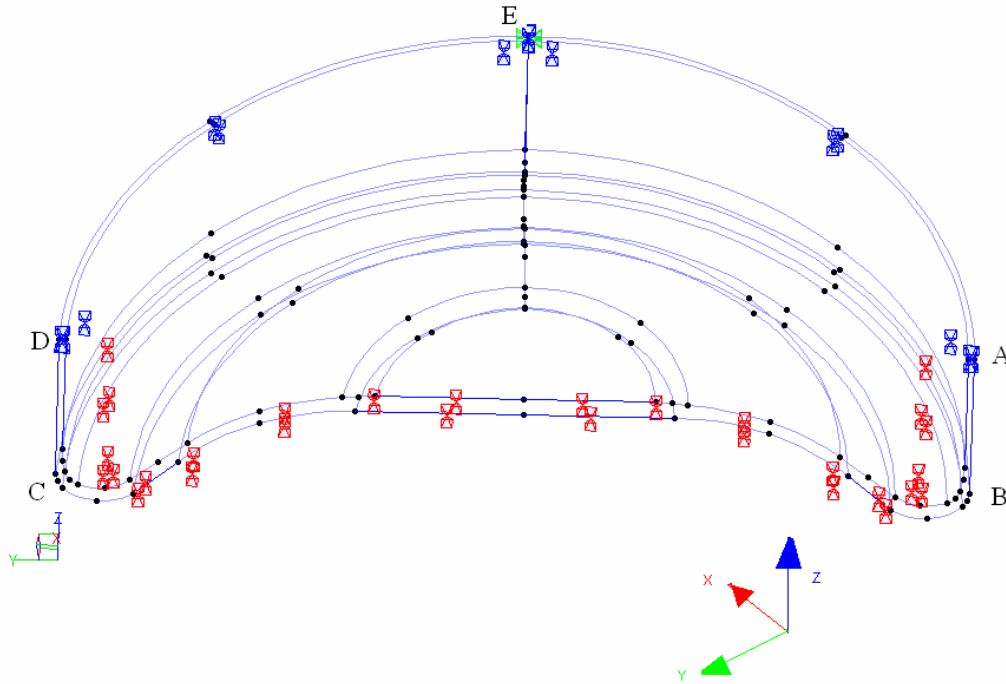


**Figure 14: Finite element model and constraints**

The multi-linear material model for aluminum 1050 is used. An incremental uniform pressure load was applied to the internal surface of the can. The mesh made up of 6315 four-noded three-dimensional elements, the finite element mesh is shown in Figure (15).

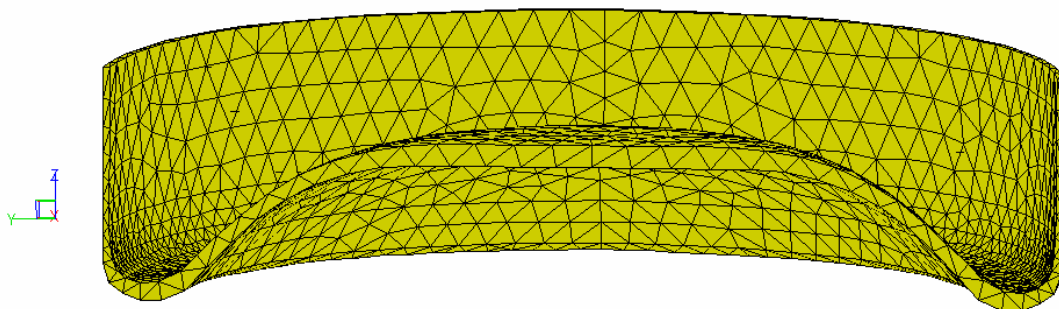


**Figure 15: 3-D Finite element model mesh**

The analysis resulted in stress contours plot for a number of incremental pressures and final Von Mises Stress is shown in Figure (16).

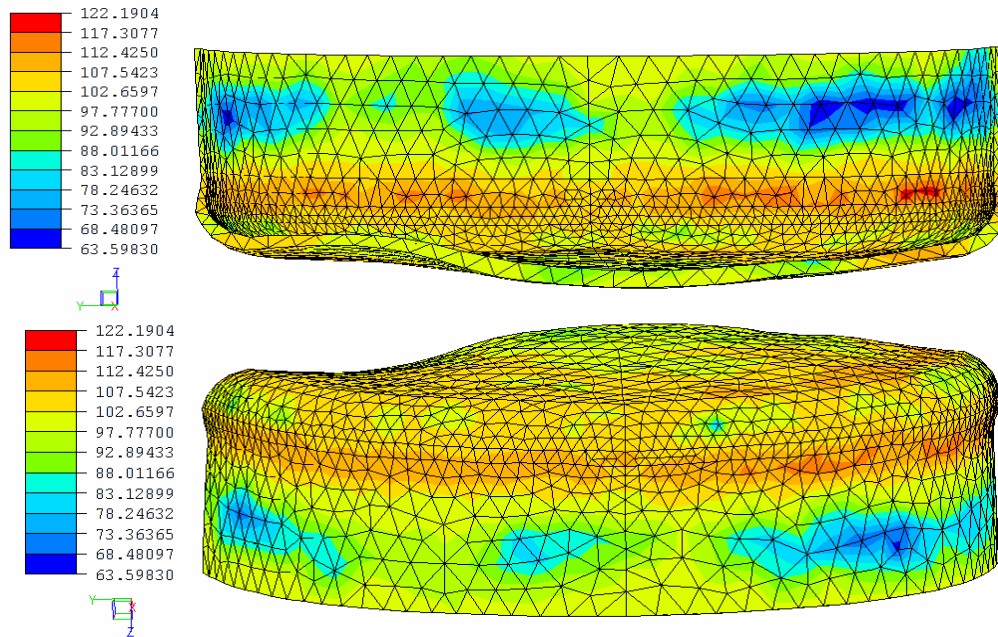


**Figure 16: Final Von Mises stress prediction at pressure of 20 bar**

## EXPERIMENTAL TESTING

Experimental pressure testing of cans having various dimensions has been done in the workshop. A typical burst can is shown in Figure (17), which also shows the buckling of the base, prior to failure. The non-symmetric nature of the deformed shape is clear and comparable with finite element predictions (see Figure (15)). There is a requirement that the buckling pressure is at least 20% below the actual burst pressure [7]. In this practical situation, minimum burst pressures are specified by the customers.



**Figure 17: Deformation and burst pressure of can base**

## DISCUSSIONS

### Results of 2-D

The can base appears to fail due to stress concentration at the radius on the outer section. It can be seen from Figure (10, 13) that in both cases there is a lot of aluminum in the centre of the base and consequently there is a region of low stress. The can base could be strengthened if aluminum is thickened at the position of the highest stress.

After the yield point, a small increase in stress causes a much large strain than before the yield point. The can base will then have large deformations as shown in figure (10, 13). The pressure is a function of volume therefore any large deformation will reduce the pressure inside the can. This cannot easily be modelled, therefore the assumption is made that the pressure in the pressure test is increased very slowly such that the water pump will prevent a reduction in pressure due increased volume.

To estimate the collapse load will increase the load until the base begins to buckle then increasing until the can walls fail, hence the model much be designed to establish the point at which the base buckles. It can be seen from figure (10) that there is a lot of aluminum in the centre of the base, which is wasted. The very low stresses at the centre of the base suggest that the can would never fail there, and would always fail at the base of the walls. Thus, the amount of aluminum in the centre of the base can be reduced, which will have no effect on the can strength unless it reaches a thickness giving an equivalent stress to that in the base of the walls. This can be improved by increasing the thickness of the outer section of the can base or changing the geometry of the can base by re-designing the bottom former. Take accurate measurements of the cans this may involve a study of the bottom to optimize their can.

### **Results of (3-D)**

The analysis resulted in stress contours plot for a number of incremental pressures. Can base yields when the internal pressure is 15 bars since the yield stress for the aluminum is 100 MPa. When the internal pressure is increased to 17 bar, significant region in the corners of the base that has yielding and will ultimately enable plastic collapse (snap-through) to occur at a pressure of 20 bar, as shown in Figure (16). The non-symmetric nature of the deformed shape is clear and comparable with finite element predictions (see Figure (16)). There is a requirement that the buckling pressure is at least 20% below the actual burst pressure [7]. In this practical situation, minimum burst pressures are specified by the customers. The results for the 53 mm can (which has been modeled here) shown very good agreement between the experimental burst pressure and finite element predictions obtained here. Similarly, the experimental buckling pressure of 1.6 MPa compares favourably with the finite element prediction of 1.7 MPa.

### **CONCLUSIONS**

This paper has described the elastic and elastic-plastic analysis of the thin cylindrical component under internal pressure loading. Initially, axisymmetric constant-thickness models have been used to investigate the stress distributions that are set up, the yield pressures and the way in which the plastic zones develop, after yielding, leading up to elastic-plastic buckling. In addition, a realistic thickness profile has been modelled in order to more accurately study the pre- and post-yield characteristics. Emphasis has been placed on the base of the cylindrical can, since this is where the major deformation occurs.

However, the axisymmetric models are not capable of distinguishing between the elastic-plastic buckling of the base and the ultimate bursting of the can. In fact, these two events are predicted to be coincident, whereas experimental evidence suggests a slightly unsymmetrical buckling mode and a clear distinction between the elastic-plastic buckling of the base and burst (collapse) pressures. A three-dimensional half-model was developed in order to investigate the elastic-plastic buckling of the base. Finite element

predictions of yield, elastic-plastic buckling and collapse (burst) pressures have been compared with experimental evidence and analytical solutions and there is generally good agreement between them.

## REFERENCES

- [1] ELFEN User Manual Version 3.0.4, Rockfield Software, Swansea, UK 1985.
- [2] Patten, S. design and optimization of aluminum aerosol cans produced by a back 2005.
- [3] Iestyn, B. J. Computational strategies for design optimization of food cans PhD, Thesis, University of Wales Swansea, 1999.
- [4] Davis, J. R. Aluminum & Aluminum Alloys, ASME International, 1993
- [5] Owen, D. R. and Hinton, J. E. NAFEMS- Introduction to Non-linear finite
- [6] Element analysis, NAFEMS, 1992.
- [7] Farshad, M. Designed and analysis of shell structures Kluwer Academic Publisher 1992.
- [8] Bushnell, D. Computerized buckling analysis of shell Martinus Nijhoff Publishers 1985.

## NOTATIONS

t	Geometry thickness
E	Elastic modulus
$\hat{i}_{eq}$	Maximum equivalent stress index
$\sigma$	Stress
$\nu$	Poisson's ratio
$\sigma^{eq}$	Maximum equivalent stress
$\rho$	Density
$\sigma_y$	Yield stress
$\sigma_1, \sigma_2, \sigma_3$	Principal stresses
$\epsilon$	Strain
G	Geometry
$P_L$	Limiting pressure
$P_c$	Collapse pressure
$\sigma_a$	Nominal stress
P	Internal pressure

## *Subscript*

a	Nominal
y	Initial yield
eq	Equivalent